Liquid–Liquid Phase Separation in Multicomponent Polymer Systems. 18. Effect of Short-Chain Branching‡

L. A. Kleintjens and R. Koningsveld*

Central Laboratory, DSM, Netherlands

M. Gordon

Department of Chemistry, University of Essex, Colchester, UK.
Received September 25, 1979

ABSTRACT: To date, polymer solution theories have failed to describe quantitatively the effect of polymer chain branching on liquid–liquid phase relationships in solution. In an attempt to improve the situation we have adapted lattice treatments to incorporate this phenomenon. A branched polymer molecule has been presented as a chain, composed of end, linear middle, and branched middle segments, each interacting through a specific surface area with the immediately surrounding molecules or segments. The expression obtained for the energy of mixing contains five parameters. They deal respectively with the degree of branching, the average length of the side chain, the interaction energy and its concentration, and temperature dependence. The values of the parameters have been obtained for polyethylene/diphenyl ether at ambient pressure by fitting the spinodal expression and the critical condition to over 100 experimental spinodal points and critical data on 35 polymer samples. The model describes spinodal, critical, and cloud-point data within experimental error over practically the full measured concentration range. Phase compositions, however, could only be reproduced qualitatively. One of the parameters in the proposed free energy expression offers a means of distinguishing between various low-density polyethylene samples with respect to the average length of the short side branches.

Branching of polymer chains plays an important role in liquid–liquid phase equilibria in polymer solutions and influences quantities like separation temperature and/or separation pressure of a polymer solution. It was shown previously for the system polyethylene/diphenyl ether that the two-phase region of a branched polyethylene solution may be shifted by more than 10 °C compared with that of a linear polyethylene sample of about equal number and mass average molar mass[1] (Figure 1). That paper also suggested an approach for dealing with the observed phase behavior in terms of a molecular model and showed that the most primitive treatment already leads to complicated expressions for the free enthalpy (Gibbs free energy) of mixing. This treatment is further explored here.

Several methods for the determination of the degree of branching in, e.g., polyethylene are available, but until now very few detailed descriptions of the effect of chain branching on thermodynamic properties have been given. Most work on branching has been done on its effect on the dimensions of the polymer molecule in solution.[2-4] However, such considerations do not allow a calculation of the chain-branching effect on the demixing behavior.

Kennedy et al.[5] generalized the Flory–Huggins free enthalpy of mixing expression to solutions of branched polymers, assigning different interaction energies to solvent–end-segment and solvent–middle-segment contacts. Through lack of experimental information, these authors were not able to calculate values for the interaction parameters.

Nakano[6] measured cloud-point curves for solutions of branched polyethylene in diphenyl ether. Using the Shultz–Flory approach,[7] he calculated the Θ temperature of the system. Instead of plotting the reciprocal liquid–liquid critical temperature against $M_w^{-1/2}$ (M_w = mass average molar mass), he used the maximum cloud-point temperature vs. the reciprocal intrinsic viscosity ($[\eta]^{-1}$). Using polyethylene samples with narrow molar-mass distributions, Nakano showed the Θ temperatures obtained from the intercept at $[\eta]^{-1} = 0$ to be equal for linear and branched polyethylene in diphenyl ether. From this he concluded that this system could be described quantitatively with an interaction parameter proportional to the long-chain-branching index g_η (g_η = the ratio of the intrinsic viscosities at the Θ temperature of branched and linear polyethylene with equal molar-mass distribution).

However, using intrinsic-viscosity measurements as experimental information, one can hardly expect to detect any influence of short side chains, which are known to constitute the larger part of the side branches in low-density polyethylene.[8] Therefore, the present model aims at incorporation of the lengths of side chains in the description of the thermodynamic behavior of polymer solutions.

Model for a Solution of a Branched Polymer

A branched polymer chain is taken to be composed of end, linear middle, and branched middle segments (Figure 2). Since polydisperse polymers are to be treated here, the polymer sample is supposed to consist of chains labeled i, differing in the number of segments m_i.

Let a fraction δ of the total number of the m_i segments of a chain i be branched middle segments, then the number of these segments per chain is $\nu_i = \delta m_i$. One or two side chains may originate from a branched middle segment; if there are two, they would generally differ in length.

Even at constant δ and m_i, the shape of branched polymer chains may be quite different; Figure 2 illustrates this. Depending on the length of the side chain, its end segments will be more or less influenced by the main chain. The shorter the side branch the less pronounced the specificity of the interaction of the end segment will be. To deal with this effect, a parameter ϵ is introduced in the model, standing for the average "effectivity" of the end segments.

The parameter ϵ will reflect overall effects of a side chain. There are as many side chains as end groups, and it will not be possible theoretically to break down the overall effect into contributions from individual units in the side chain. For very short side chains, the effectivity will be much less than unity ($0 < \epsilon \ll 1$; Figure 2a). With growing side-chain length, the effectivity of the end segment will rapidly go to unity and remain constant from thereon ($\epsilon = 1$; Figure 2b). The total *effective* number of

‡ Dedicated to professor Walter H. Stockmayer on the occasion of his 65th birthday.

0024-9297/80/2213-0303$01.00/0

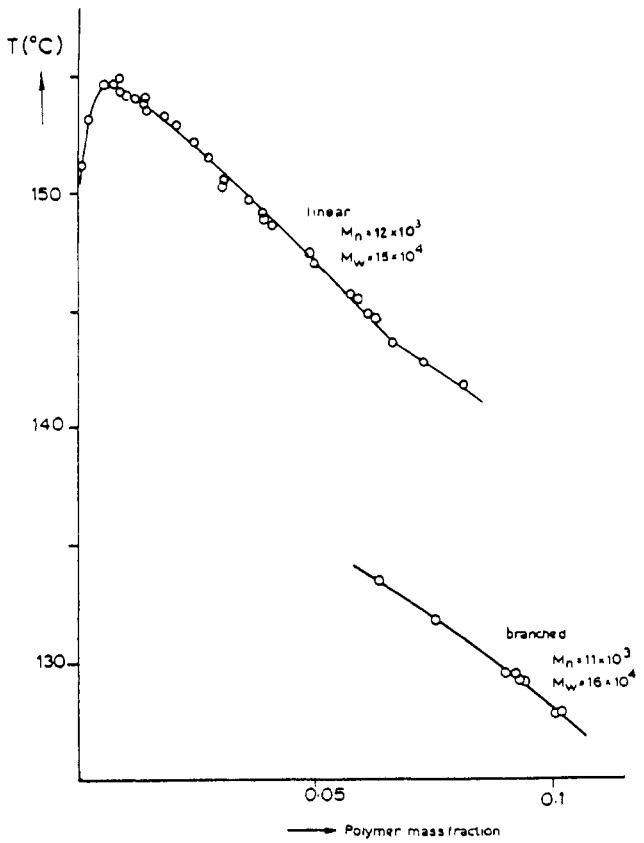

Figure 1. Cloud-point curves in diphenyl ether of linear and branched polyethylene of about equal number- and mass-average molar mass.

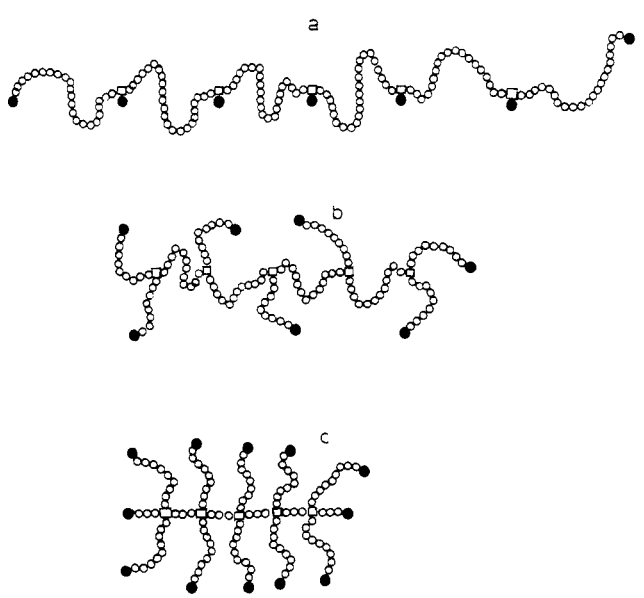

Figure 2. Illustration of several types of branched polymer chains, equal in number of segments (m_i) and number of branch points (δm_i) but differing in length of side chains (ϵ, see text) and functionality of branch points: chain a, $0 < \epsilon \ll 1$; chain b, $\epsilon = 1$; chain c, $\epsilon = 2$.

end segments per chain i is thus: $2 + \epsilon\nu_i$. If two side branches originate from a branched middle segment the value of ϵ will be between 0 and 2 for such branched middle segments (Figure 2c).

To make the model somewhat more general, we divide the solvent molecule into s_0 segments. The number of segments m_i per chain can be calculated from

$$m_i = cs_0M_i \tag{1}$$

where $c = v_p/v_0M_0$, v_p and v_0 are the specific volumes of the solvent and the polymer in solution, and M_0 and M_i are the molar masses of solvent and polymer species i, respectively. In the following calculations, average values of m will arise, viz., the number (m_n), mass (m_w), and z (m_z) averages, defined in the usual way.

For the numbers of the various kinds of segments in the system we have

$$N_s = n_os_o \qquad N_e = \sum n_i(2 + \epsilon\nu_i) \qquad N_b = \sum n_i\nu_i$$
$$N_m = (\sum n_im_i) - (N_b + N_e) = \sum n_i\{m_i - 2 - \nu_i(1 + \epsilon)\} \tag{2}$$

where N_s is the number of solvent segments, N_e is the effective number of end segments, N_b is the number of branched middle segments, N_m is the number of linear middle segments, and n_o and n_i are the numbers of solvent and of polymer molecules i, respectively.

Gibbs Free Energy of Mixing

The interaction energy belonging to a contact of a pair of segments depends on their nature. One can account for this by giving each kind of contact a specific interaction energy. It was suggested long ago by Staverman[9] and has been shown clearly in the newer work of Huggins[10] and Flory[11] that the *contact surface area* of interacting segments plays an important role. Instead of having a fixed number of interacting neighbors (i.e., the lattice coordination number) each segment is given an interacting surface area σ.[12,13] The energy involved in a contact is now calculated by multiplying the contact surface area with the interaction energy per unit contact surface area. A similar improvement has been suggested by Rowlinson[14a] and by Kanig.[14b]

Substituting the number of intermolecular contacts of a segment j by its specific contact surface area σ_j, we obtain for the total interacting surface areas N_0, N_1, N_2, and N_3 of the various types of segments:

$$N_0 \equiv s_0n_0\,\sigma_0 = \sigma_0\varphi_0N_\varphi \tag{3a}$$

$$N_1 \equiv \sigma_1\sum n_i(2 + \epsilon\nu_i) = (\epsilon\delta + 2m_n^{-1})\sigma_1\varphi N_\varphi \tag{3b}$$

$$N_2 \equiv \sigma_2\sum n_i\{m_i - 2 - \nu_i(1 + \epsilon)\} = \{1 - \delta(1 + \epsilon) - 2m_n^{-1}\}\sigma_2\varphi N_\varphi \tag{3c}$$

$$N_3 \equiv \sigma_3\sum n_i\nu_i = \delta\sigma_3\varphi N_\varphi \tag{3d}$$

$$N = N_\varphi[\varphi_0\sigma_0 + \varphi\{\sigma_1(\epsilon\delta + 2m_n^{-1}) + \sigma_2(1 - \delta - \delta\epsilon - 2m_n^{-1}) + \sigma_3\delta\}] \tag{3e}$$

where σ_0, σ_1, σ_2, and σ_3 are the specific contact surface areas of solvent (0), end (1), linear middle (2), and branched middle segments (3), respectively, and $N_\varphi = n_0 + \sum n_im_i$. Thus we find

$$\sigma = \sigma_1(\epsilon\delta + 2m_n^{-1}) + \sigma_2\{1 - \delta(1 + \epsilon) - 2m_n^{-1}\} + \sigma_3\delta \tag{3f}$$

for the mean contact surface area of a whole chain.

Within the model the concentrations of solvent and whole polymer are represented by volume fractions defined by

$$\varphi_0 = n_0s_0/N_\varphi; \qquad \varphi = (\sum n_im_i)/N_\varphi \tag{3g}$$

We rewrite $N_\varphi = N(\varphi_0\sigma_0 + \varphi\sigma) = (1 - \gamma\sigma)\sigma_0N_\varphi$ and thus define an important parameter γ:

$$\gamma = 1 - (\sigma/\sigma_0) = 1 - \rho \tag{4}$$

Application of the random distribution assumption (strictly regular solution model[15]) leads to the following expression for the numbers P_{jk} of contact pairs in the mixture

$$P_{jk} = N_j\theta_k \text{ (for } j \neq k\text{); and } P_{jj} = \tfrac{1}{2}N_j\theta_j \quad (5)$$

where $\theta_k = N_k/N$.

The enthalpy of mixing ΔE_{mix} is defined as the total change in interaction energy caused by a change in the numbers of contact pairs upon mixing n_0 solvent molecules with $\sum n_i$ polymer chains. Denoting the numbers of contact pairs in the constituents by P^0_{jk} we find

$$\Delta E_{mix} = \sum_j \sum_k (P_{jk} - P^0_{jk})w_{jk} \quad (6)$$

where w_{jk} is the interaction energy involved per unit contact area of segments j and k. Combination of eq 3, 5, and 6 yields

$$\Delta E_{mix}/RTN_\varphi = g\varphi_0\varphi \quad (7)$$

where g is defined by

$$RTg = (1 - \gamma\varphi)^{-1}[(\delta\epsilon + 2m_n^{-1})\sigma_1\Delta w_{01} + \{1 - \delta(1 + \epsilon) - 2m_n^{-1}\}\sigma_2\Delta w_{02} + \delta\sigma_3\Delta w_{03} - \sigma_1\sigma_2\sigma^{-1}\{1 - \delta(1 + \epsilon) - 2m_n^{-1}\} \times (\delta\epsilon + 2m_n^{-1})\Delta w_{12} - \sigma_1\sigma_3\sigma^{-}(\delta\epsilon + 2m_n^{-1})\delta\Delta w_{13} - \sigma_2\sigma_3\sigma^{-1}\{1 - \delta(1 + \epsilon) - 2m_n^{-1}\}\delta\Delta w_{23}] \quad (8)$$

and $\Delta w_{jk} = w_{jk} - {}^1/_2(w_{jj} + w_{kk})$.

Within the model this is a very general expression for ΔE_{mix}, and it contains ten system-dependent adaptable parameters, viz., σ_0, σ_1, σ_2, and σ_3 and Δw_{01}, Δw_{02}, Δw_{03}, Δw_{12}, Δw_{13}, and Δw_{23}. The situation shows a complexity comparable to that which resulted from the considerations of Kennedy et al.[5] However, without serious loss of generality, one could considerably simplify the equation taking the interaction energy per unit contact surface area for all kinds of polymer segments with respect to solvent segments to be equal ($\Delta w_{01} \equiv \Delta w_{02} \equiv \Delta w_{03} \equiv \Delta w_{op}$). Again, it would then seem logical to neglect the interaction energies between the various segments in the polymer ($\Delta w_{12} = 0$, $\Delta w_{13} = 0$, and $\Delta w_{23} = 0$).

After these two simplifying assumptions, eq 8 reduces to

$$RTg = \sigma\Delta w_{op}/(1 - \gamma\varphi) = \sigma_0(1 - \gamma)\Delta w_{op}/(1 - \gamma\varphi) \quad (9)$$

and eq 7 to

$$\Delta E_{mix}/N_\varphi RT = g_{op}(1 - \gamma)\varphi_0\varphi/(1 - \gamma\varphi) \quad (9a)$$

where $g_{op} = \sigma_0\Delta w_{op}/RT$. With the abbreviation $\rho_k = \sigma_k/\sigma_0$, the expression for γ (eq 4) can be changed into

$$\gamma = 1 - \rho_2 - (\rho_3 - \rho_2)\delta - (\rho_1 - \rho_2)(\epsilon\delta + 2m_n^{-1}) \quad (10)$$

Interaction parameters usually show an at least approximately linear dependence on reciprocal absolute temperature[16] ($g_{op} = g_1 + g_2/T$) so that we finally retain five adaptable parameters, viz., ρ_1, ρ_2, ρ_3, g_1, and g_2.

Following the usual procedure, we can now formulate the free enthalpy of mixing ΔG adding appropriate terms for the combinatorial entropy of random mixing to eq 9a. We choose the lattice expression devised independently by Flory,[17] Huggins,[18] and Staverman and van Santen[19] and obtain

$$\Delta G/N_\varphi RT = \varphi_0 s_0^{-1} \ln \varphi_0 + \sum \varphi_i m_i^{-1} \ln \varphi_i + g_{op}(1 - \gamma)\varphi_0\varphi/(1 - \gamma\varphi) \quad (11)$$

Experimental Methods

To obtain the parameters in free enthalpy of mixing expressions for polymer solutions, several techniques have been developed for both very dilute polymer solutions and for concentrated polymer systems. Since there is no way of determining ΔG as such, all methods are based on the determination of derivatives of ΔG, e.g., with respect to concentration. Usually interaction parameters are optimized by fitting expressions for such derivatives to a set of experimental data on a series of well-characterized polymer samples.

In this work three types of data are used, viz., liquid-liquid critical points, spinodal points, and phase compositions after phase separation. The adopted procedure consists of a fitting of spinodal and critical points to free enthalpy expression 11 and a subsequent prediction of liquid-liquid phase relationships.

1. Spinodal Points. According to Gibbs,[20] the spinodal condition (or limit of thermodynamic stability) for a liquid multicomponent system is given by

$$J_{sp} = |\partial^2\Delta G/\partial\varphi_i\,\partial\varphi_j|_{p,T} = 0 \quad (12)$$

where φ_i and φ_j stand for the independent concentration variables, in this case the volume fractions of all polymer species present.

Application of eq 12 to eq 11 yields[21]

$$(1/\varphi_0 s_0) + (1/\varphi m_w) - 2(1 - \gamma)^2(1 - \gamma\varphi)^{-3}g_{op}(T) = 0 \quad (13)$$

an expression for the spinodal that relates experimentally accessible quantities (φ_0, φ, m_w, T) to the set of interaction parameters (γ, $g_{0p}(T)$) or (ρ_1, ρ_2, ρ_3, g_1, g_2). The φ_i dependence of γ, expressed in eq 10 by the term $2/m_n$, was neglected in the derivation. It can be shown that this simplification has no significant influence on the values of the parameters.

Determination of the spinodal temperature for a given concentration is a method that has come to the fore in recent years. Based upon well-established considerations about the origin of light scattering by homogeneous liquid mixtures,[22-25] the method relates the reciprocal light intensity $I(0)$ scattered at zero scattering angle to the determinant defined in eq 12 in direct proportionality. Therefore, upon reaching the spinodal temperature, $I(0)$ will diverge and a plot of $I(0)^{-1}$ vs. T can be used to locate the spinodal temperature by extrapolation.

This principle has been successfully applied by various authors (see ref 26 and 27), and we have employed it here in the variant developed in recent years by Gordon et al.[28-30] The latter method, called Pulse Induced Critical Scattering (PICS), makes use of the short supercooling demixing polymer solutions usually allow before separating into two liquid phases. By application of thermal cooling pulses, followed by heating steps up to the one-phase region, meta-stable one-phase states can be realized long enough for scattering intensity readings to be taken. The PICS technique allows a closer approach to the spinodal than the conventional static method.

For convenience the intensity is measured at two fixed angles only (30 and 90°); usually we measured at 30°. It has been checked with the system polystyrene/cyclohexane that the spinodal temperatures determined in this way are consistent with those obtained by the conventional procedure.[31] Figure 3 shows some representative PICS results on the system polyethylene/diphenyl ether at stated overall polymer concentrations (close to the critical, 9.3 wt %) and their extrapolation to the spinodal temperature. The values obtained can be seen to be quite accurate (±0.1 °C).

2. Liquid-Liquid Critical Point. Gibbs[20] also formulated a condition for the liquid-liquid critical state which, applied to eq 11, yields[21]

$$(1/s_0\varphi_{0c}^2) - (m_z/m_w^2\varphi_c^2) - 6\gamma(1 - \gamma)^2(1 - \gamma\varphi_c)^{-4}g_{op}(T) = 0 \quad (14)$$

where φ_c (=1 − φ_{0c}) is the critical whole-polymer concentration.

The exact position of a critical point on the cloud-point curve can be simply and accurately located by measurement of the phase-volume ratio for a given concentration as a function of temperature.[32,33]

3. Analysis of the Phases. One of the oldest methods for gaining thermodynamic information on partially miscible systems is the analysis of the phases after a liquid-liquid separation. With polymer solutions, this situation is complicated by the unavoidable fractionation which causes the polymer fractions to differ in molar-mass distribution. Consequently, the full characterization of the phases has always been a tedious job[34-36] until the advent of gel permeation chromatography which made the determination of molar-mass distributions almost a routine matter for linear polymers.

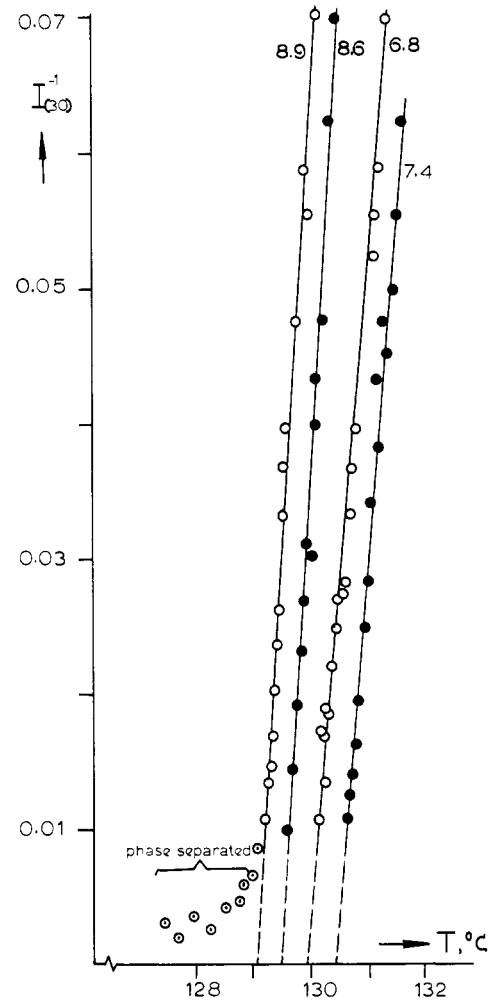

Figure 3. Experimental PICS intensity measurements at scattering angle 30° (I_{30}) extrapolated to the spinodal temperature for indicated polymer concentrations of sample 2 (in mass percent) in diphenyl ether.

We did carry out such an analysis, augmented by on-line viscometry and low-angle laser light scattering to detect and determine long-chain branching, but defer a detailed analysis to a later paper. Here we only use the whole polymer concentrations of the phases which can be plotted in a quasibinary phase diagram showing the dependence of the location of coexistence curves on the whole polymer concentration of the system.[32,37]

Such diagrams can also be calculated from a suitable free enthalpy of mixing function, which amounts to equating the values of the chemical potentials of each component in the two phases. For systems obeying the ΔG function 11 the chemical potential differences $\Delta\mu_k$ between the dissolved and the pure component liquid state read

$$\Delta\mu_0/s_0RT = s_0^{-1} \ln \varphi_0 + [(1/s_0) - (1/m_n)]\varphi + \varphi^2(1 - \gamma)^2(1 - \gamma\varphi)^{-2}g_{op} \quad (15)$$

$$\Delta\mu_i/m_iRT = m_i^{-1} \ln \varphi_i + [(1/s_0) - (1/m_n)]\varphi - (1/s_0) + (1/m_i) + \varphi_0^2(1 - \gamma)(1 - \gamma\varphi)^{-2}g_{op} \quad (16)$$

for solvent and polymer species i, respectively. A numerical procedure for dealing with such equations has been outlined elsewhere.[40]

The analysis of the phases has been carried out as follows. Overall polymer concentration and separation temperature are chosen in such a way that one obtains a phase-volume ratio between 0.1 and 10. Polymer and solvent are weighed into a glass tube which is sealed under vacuum while the system is frozen in liquid nitrogen. The mixture is homogenized by vibrating the tube at a temperature above the cloud point and, while vibrating the system, it is cooled down to the desired separation temperature. The vibrator is stopped after 10 min and the phases are allowed to segregate. After this process is complete, the phase-volume ratio is measured and the system quenched in liquid nitrogen. Both phases solidify without appreciable change in composition, and they can easily be separated by breaking the solid mixture along the original liquid-liquid phase boundary.[38]

Table I
Molecular Characterization of the Polyethylene Samples

sample no.	M_n, kg/mol	M_w	M_z	D, end groups/100 C
1	23	247	2000	2.36
2	11	160	1800	2.34
3	8.5	70	660	2.48
4	18	45	490	2.29
5	14	70	550	2.21
6	64	345	2900	2.33
7	34	230	1650	2.30
8	65	420	2900	2.23
9	12	150	900	linear
10	92	140	270	linear
11	8.6	55	300	linear
12	8	177	990	linear
13	7.9	89	730	linear
14	200	680		linear
15	15	27.5	99	linear
16	19	36	126	linear
17	38	550		linear
18	34	150	286	linear
19	17	274		1.80
20	38	640		2.41
21	19	229		1.20
22	24	470		0.75
23	27	420		1.38
24	29	219		1.46
25	7	54		5.18
26	8.4	32		5.26
27	19	84		1.42
28	30	525		2.21
29	25	385		2.31
30	35	375		2.18
31	29	165		2.25
32	31	800		2.45
33	24	123		2.83
IUPAC B	25	600		1.63
HPBD	48	52		2.05

The System Polyethylene/Diphenyl Ether

To check whether the Gibbs free energy relation derived above (eq 11) is capable of describing actual polymer solution behavior, polyethylene is chosen as a model polymer with branched chains. Characterization techniques for molar-mass distribution and end-group concentration have been well developed for this polymer.[39] As there is a broad variety of polyethylene types being manufactured nowadays, it is not too difficult to obtain samples differing widely in degree of branching.

Diphenyl ether is known as a Θ solvent for polyethylene, with a Θ temperature far enough above the crystallization temperature of polyethylene in solution to allow measurements of liquid-liquid phase equilibria including critical points on a range of molar masses.

The characterization data on the samples used are given in Table I, where D stands for the mean number of end groups per 100 carbon atoms in the polymer chain. Liquid-liquid critical points, measured with the phase-volume ratio method, are listed in Table II and are expressed as volume fractions calculated from mass fractions and densities assuming ideal volume mixing.

Spinodal temperatures determined by PICS were measured on four samples (samples 1, 2, 5, and 7 in Table I). In all cases the reciprocal of the scattering intensity at 30° proved to be linear in temperature (examples in Figure 3). Only at temperatures close to the spinodal may phase

Table II
Critical Concentrations and Temperatures in Diphenyl Ether for the Samples of Table I

sample no.	φ_c	T_c, K	sample no.	φ_c	T_c, K
1	0.083	409.0	19	0.084	409.2
2	0.113	402.4	20	0.0695	409.8
3	0.188	387.0	21	0.084	410.2
4	0.115	399.0	22	0.086	410.6
5	0.10	403.6	23	0.085	409.9
6	0.061	413.1	24	0.075	412.3
7	0.068	411.3	25	0.139	385.4
8	0.050	415.3	26	0.133	384.7
9[a]	0.082	416.2	27	0.089	408.1
10[a]	0.050	421.9	28	0.074	411.4
11[a]	0.097	410.1	29	0.084	408.4
12	0.076	417.8	30	0.067	412.6
13	0.106	411.2	31	0.074	410.0
14	0.030	427.8	32	0.075	410.9
15	0.099	405.0	33	0.121	396.7
16	0.116	406.6	IUPAC	0.084	408.8
17	0.0667	419.5	HPBD	0.0592	411.2
18	0.0556	420.6			

[a] Reported in ref 32.

separation (demixing) occur before thermal equilibrium is reached and the relevant scattering data are discarded. The probable error in the spinodal temperatures will be 0.1–0.2 °C for these highly polydisperse systems at relatively high temperature. The accuracy of the overall polymer concentration, expressed as volume fraction, is estimated to be ±0.002; errors arise mainly from evaporation because polyethylene solutions had to be injected into PICS capillaries at 160 °C in order to prevent phase separation during the filling.

Phase separations followed by complete analysis of the phases were carried out with sample 1. Establishment of complete separation, determined by accurate measurements of the phase volumes, was reached in 2 days. After allowing an extra day of separation time, the system was analyzed as described above and in ref 38. Separation temperature and overall polymer concentration were varied to check their influence on the miscibility relations; Table III lists the results.

Interaction Parameters for Polyethylene/Diphenyl Ether

Writing the critical condition (eq 14) as

$$Y \equiv \{(1/s_0\varphi_{0c}^2) - (m_z/m_w^2\varphi_c^2)\}/6 = \gamma(1-\gamma)^2(1-\gamma\varphi_c)^{-4}g_{op} \quad (17)$$

and the spinodal expression (eq 13) as

$$X \equiv \{(1/s_0\varphi_0) + (1/m_w\varphi)\}/2 = (1-\gamma)^2(1-\gamma\varphi)^{-3}g_{op} \quad (18)$$

we deduce two relations between experimentally accessible quantities and adjustable parameters. Since the critical point is also a spinodal point, both relations must hold for the critical data. Combination of eq 17 and 18 leads to an expression for γ that contains only experimental quantities

$$\gamma = Y/(X + \varphi_c Y) \quad (19)$$

Details of the fitting procedure have been reported elsewhere,[1,40] and we shall therefore only give an outline here and note some general problems.

In principle, eq 19 can be used to calculate the γ value for each sample from its critical concentration φ_c and m_w and m_z values. Because the latter quantity in particular is subject to considerable experimental uncertainty, great precision cannot be reached in this way. Apart from that, there is the basic problem of the form of eq 10 which relates γ to molecular parameters. If the latter were known, eq 10 could be fitted to the above mentioned set of γ values. For δ we have

$$\delta = (D/1400cs_0) - (2/m_n) \quad (20)$$

where D is the number of end groups per 100 carbon atoms; m_n does not pose a problem either. Compared with the polyethylene segments, the diphenyl ether molecules are rather bulky. To account for this we arbitrarily set $s_0 = 2$.

However, there is no way to obtain independent information on ϵ that the authors are aware of and hence determination of the surface–area ratio ρ_i is not feasible in this manner. An additional assumption must be made referring to either ϵ or ρ_3, since these parameters cannot be separated in an optimization involving eq 10 or 17 and 18. We have chosen ϵ, thus obtaining the better fits, and consider ϵ as a relative quantity of which we know at least that its value must lie between 0 and 2.

To avoid uncertainties due to γ as much as possible, we first analyze the data on linear samples. For these $\delta = 0$, and the concentration of end groups is small. The γ values calculated with eq 19 can be represented by $\gamma = 0.11 + m_n^{-1}$ and are introduced into eq 18, which yields $g_{op}(T)$. Figure 4 shows that the usual linear dependence on T^{-1} is well obeyed (temperature range about 25 Centigrade degrees). It is possible to check on the g_1 and g_2 values of −0.309 and 271, thus obtained, by comparing the Flory

Table III
Experimental r Value of Diphenyl Ether/Polyethylene (Sample 1) and Phase Compositions at Several Temperatures and Overall Polymer Concentrations (Expressed in Mass Percent; Estimated Uncertainty 0.2%)

temp, °C	overall concn	r value	phase concn	
			concnd	dilute
132.0	3.994	4.564	13.7	2.2
133.0	3.979	4.578	11.9	2.1
134.0	4.013	4.583	11.7	2.5
135.0	4.074	4.507	12.3	2.6
136.0	3.995	4.653	10.3	2.9
137.0	3.977	5.162	9.2	2.9
138.0	3.994	6.142	8.1	3.3
132.0	5.990	2.208	12.6	3.0
133.0	5.986	2.154	11.5	3.4
134.0	5.983	2.155	11.4	3.0
135.0	5.970	1.877	10.4	3.9
136.0	5.990	1.820	9.7	4.0
132.0	7.009	1.508	10.7	3.5
133.0	7.010	1.440	10.7	3.7
134.0	6.985	1.397	10.7	3.9
135.0	6.945	0.887	9.2	4.6
135.0	1.001	29.6	12.5	0.88
140.0	1.00	⩽40		0.89

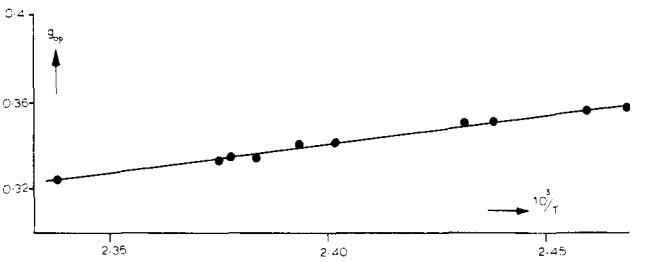

Figure 4. Temperature dependence of the interaction parameter g_{op} obtained from a least-squares fit of the critical points of the linear polyethylene samples in diphenyl ether, described by $g_{op} = -0.309 + 271/T$.

Θ temperature they imply with literature values. The Θ state can be defined either by a zero value of the osmotic second virial coefficient, implicitely defined by eq 15, or by setting $\varphi_c = 0$ and $m_w = \infty$ in the spinodal eq 18. Either procedure yields

$$g_{op}(\Theta)(1 - \gamma_{m=\infty})^2 = (1/2s_0) \quad (21)$$

which, for $s_0 = 2$ and $\gamma_{m=\infty} = 0.11$, leads to Θ = 160.8 °C. Literature[6,32,41,42] cites values of 160.3, 161.7, 164.2, and 161.5 °C, and we consider the g_1 and g_2 values obtained here to be satisfactorily consistent with them.

As explained above, a reference value must be chosen for ϵ to deal with the branched samples. We selected IUPAC LDPE sample B for the purpose and arbitrarily set $\epsilon = 1$ for this standard material. A value of ϵ deviating from 1 will indicate that, within the scope of the model, the relevant sample has on the average shorter or longer "short-chain" branches than the reference polymer. In order to carry out an optimization we need more data and turn to samples 1 (whole polymer) and 2 to 8 (fractions prepared from it). Spinodal points having been determined for samples 1, 2, 5, and 7, they can be added, and the γ values derived from eq 18 (with the g_1 and g_2 values from the linear-sample data) can be optimized to eq 10 written as

$$\gamma = C_1 + C_2\delta + C_3(\epsilon\delta + 2m_n^{-1}) \quad (22)$$

provided ϵ values are introduced for every single sample.

In the present model of a polymer chain the effectivity ϵ of an end segment is taken independent of the length of the main chain. Since samples 2 to 8 were obtained by a liquid–liquid fractionation of sample 1[40] it seems reasonable to assign the same value of ϵ to samples 1 to 8. In other words, the fractionation is assumed to have operated via molar mass only.

The best description of the critical data of samples 1–18 and IUPAC LDPE standard B (with $\epsilon = 1$) as well as the spinodal data on samples 1, 2, 5, and 7 proved to be obtained setting $\epsilon = 0.86$ for samples 1–8. We then find $C_1 = 0.1118 \pm 0.0009$, $C_2 = -0.3965 \pm 0.0546$, and $C_3 = 0.6740 \pm 0.0629$. Spinodals calculated with this set of values are shown in Figure 5 to be in fair agreement with the measured points.

Parameters obtained by an optimization procedure are often heavily correlated, and it is difficult to give them individually a precise physical interpretation. Nevertheless, one could calculate the contact surface–area ratio from the coefficients in eq 22 and see whether the results are within the tolerances imposed by the model. If we set the contact surface area of a solvent segment equal to unity, we obtain $\sigma_1 = 0.2$ (end segments), $\sigma_2 = 0.9$ (linear middle segments), and $\sigma_3 = 1.2$ (branched middle segments), values within the order of magnitude one would estimate.

At low polymer concentration calculated and experimental spinodals deviate. Such an effect was found earlier for the system polystyrene/cyclohexane and could be attributed to the non-uniform segment density in solutions at concentrations where there is little overlap of polymer coils.[31,38,44] Although moderate success has been achieved in the development of a free enthalpy function describing both dilute and concentrated regimes, a full quantitative treatment for linear chains is still lacking at this time. We have to leave the problem here merely noting that branched chains evidently give rise to a similar situation.

So far we have achieved nothing but a not too elegant curve fitting of data on the basis of a highly simplified model and additional assumptions. Further justification is obviously needed and could be given by checking the predictive value of the equations obtained. To this end we compare in the next section calculated and measured phase relationships.

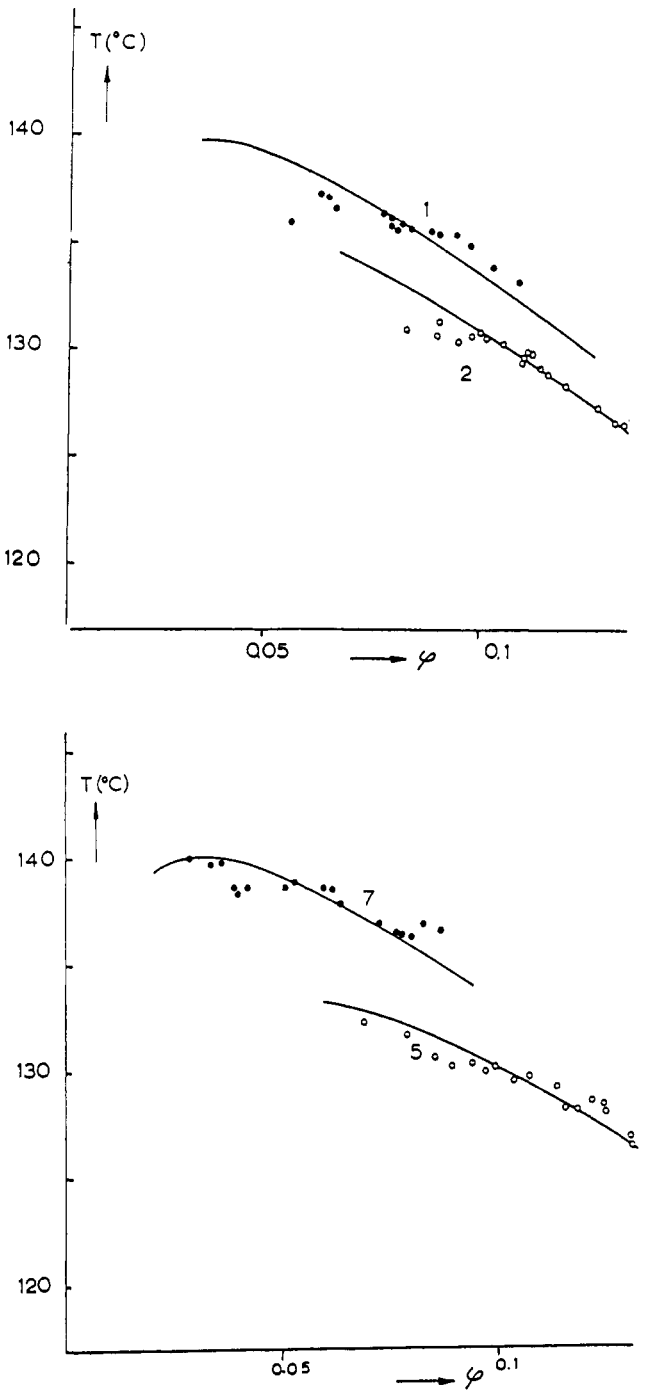

Figure 5. Comparison of experimental (●, ○) and calculated spinodals for indicated samples in diphenyl ether; (—) calculated with the parameters from a fit of all spinodal points and 18 critical points (see text).

Some practical value adheres to the outlined procedure, however. All parameters except ϵ having been determined one can now use the critical or a spinodal point to estimate ϵ for an arbitrary sample of polyethylene and refer the average length of its short side chains to that of the standard material. We did so with samples 19–33 and found ϵ values ranging from 0.84 to 1.32 (Table IV). Within the scope of the model one might conclude that the average numbers and the average overall lengths of the short side chains may differ appreciably. Samples with a large relative number of short side chains show a small

Table IV
ϵ Values Calculated from the Experimental Critical Points with Eq 18[a]

sample no.	ϵ	sample no.	ϵ
19	0.888	28	0.850
20	0.897	29	0.855
21	0.992	30	0.837
22	1.315	31	0.836
23	0.997	32	0.838
24	0.888	33	0.939
25	0.840		
26	0.832	HPBD	0.685
27	0.876		

[a] For the interaction parameters in γ, the values obtained from the fit of all spinodal points were used.

value of ϵ. Values of ϵ exceeding unity may be interpreted as indicating the presence of tetrafunctional branched middle segments.

NMR analyses of branched polyethylene have revealed that there is a distribution of short side-chain lengths ranging from ethyl to amyl groups.[8] Very long branches also exist as is clearly indicated by intrinsic viscosity vs. molar mass plots. The present method can only indicate the average length of the branches and may find a useful practical application in allowing relative comparisons between the samples in sets of low-density polyethylenes.

To verify the reliability of the procedure in this respect we checked whether a polyethylene sample with known very short side branch structure would indeed arise from the analysis with a small value for ϵ. A sample of polyethylene having ethyl side chains only can be prepared by hydrogenation of anionically polymerized butadiene.[43] The main process of 1–4 addition is accompanied by some 1–2 addition which, upon hydrogenation of the product, leads to a polyethylene chain carrying ethyl branches. Sample HPBD has been prepared in this way and indeed shows the lowest ϵ value found so far (Table IV).

Measured and Predicted Phase Diagrams

A two-dimensional phase diagram for a polydisperse polymer solution shows various curves.[32] We have the cloud-point curve obtainable by extrapolation of phase-volume ratios at various whole-polymer concentrations to either zero or infinity, depending on whether the overall polymer concentration is larger or smaller than the critical one. A less elaborate way is the direct turbidimetric determination of the cloud point for a given concentration.[32]

Every overall concentration corresponds with a coexistence curve composed of two branches representing the overall concentrations of the two phases as a function of the separation temperature. Only for monodisperse polymer samples are all coexistence curves bound to coincide and be identical with the cloud-point curve.

Coexistence curves can be obtained experimentally from a series of phase separations at constant overall polymer concentration, followed by analysis of the phases (see above). Sample 1 was selected for the comparison and subjected to such a series of separations in diphenyl ether. Table III lists the data collected; Figure 6 shows the experimental phase diagram.

To check the consistency of the present treatment we calculate the phase diagram for sample 1, using the values for δ and ϵ given above and the absolute molar mass distribution obtained by gel permeation chromatography combined with on-line low-angle laser light scattering. The distribution was approximated by a set of 25 δ functions shown in Figure 7. The critical point was calculated with eq 20 and the phase equilibria with eq 15 and 16 (set of

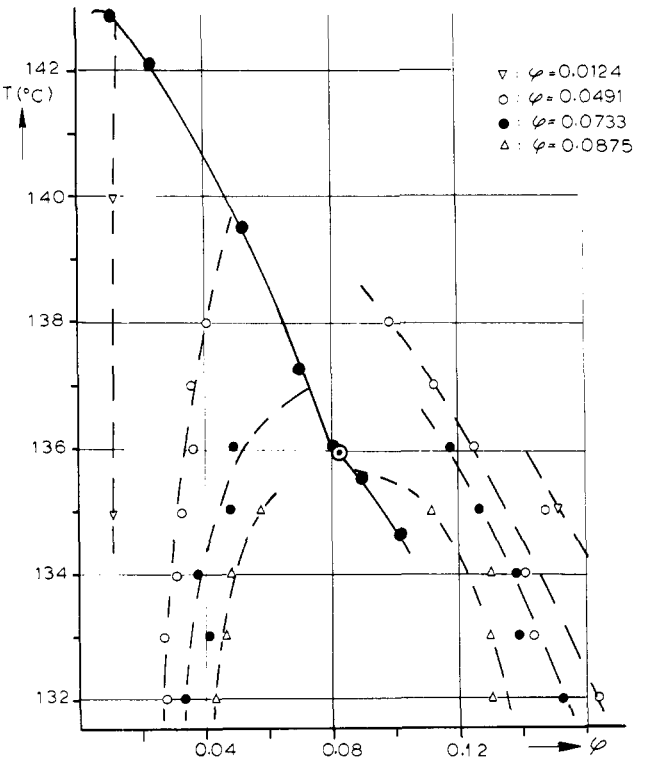

Figure 6. Experimental phase diagram of sample 1 in diphenyl ether: (---) coexistence curves for indicated overall polymer volume fractions; (-●-) cloud-point curve from the Turbidimeter; (⊙) critical point.

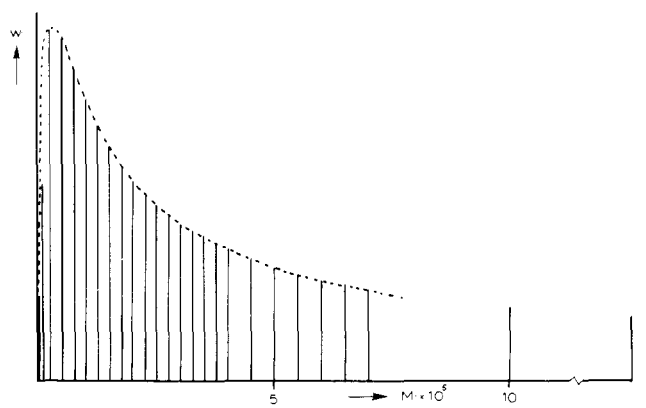

Figure 7. Representation of the molar mass distribution of sample 1 (---), by a series of delta functions, used in the calculation of Figure 8.

26 equations). Figure 8 shows the calculated phase diagram which proves to agree quite well with the experimental one.

Discussion

A closer scrutiny of Figures 6 and 8 reveals that there are small but significant differences in the phase concentrations. This might be attributed to the dilute-solution effects mentioned before, and a further study of the phenomenon is obviously needed in order to achieve quantitative agreement. On the whole, however, we consider the proposed model a useful one, not only because of the semiquantitative agreement between the phase diagrams, but also because the shift of the ϵ value, expected for the HDPB sample on physical grounds, is correctly produced.

The model necessarily leads to a complex free enthalpy equation because the system is complicated. The utmost simplification still leaves us with five adjustable parameters

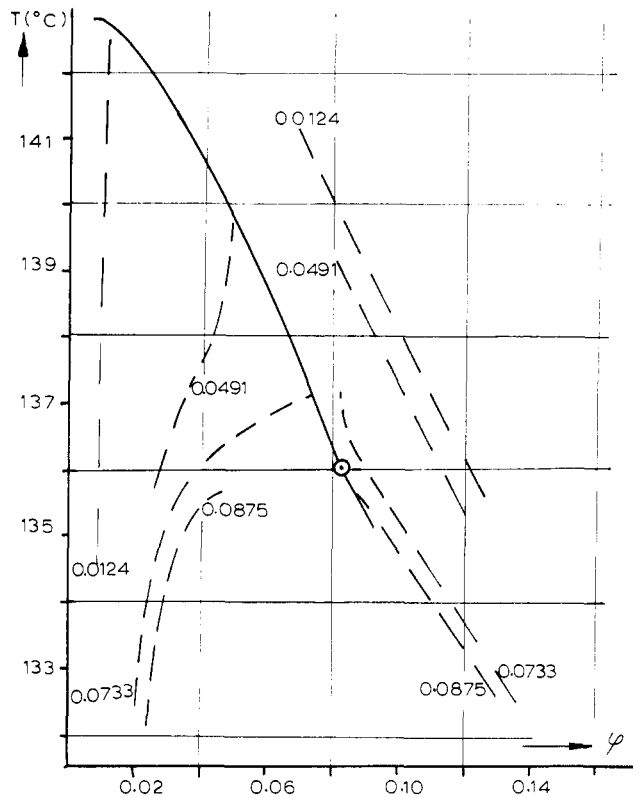

Figure 8. Phase diagram, calculated for sample 1 in diphenyl ether: (- - -) coexistence curves for indicated overall polymer volume fractions, (—) cloud-point curve; (⊙) calculated critical point.

for the determination of which over 100 spinodal points and 18 critical points were used. This represents an amount of work which detracts from the applicability of the procedure.

Apart from the dilute-solution effect there are other problems still to deal with. Combination of eq 10 and 21 yields

$$g_{op}(\Theta)[1 - \{1 - \rho_2 - (\rho_3 - \rho_2)\delta - (\rho_1 - \rho_2)\epsilon\delta\}] = (1/2s_0) \quad (23)$$

which implies that the model predicts a dependence of the Flory temperature on the number and effective length of the short side chains. This suggested effect does not necessarily contradict Nakano's conclusion that the Θ temperature is independent of long-chain branching.[6] Nakano's data are well represented for linear and branched polyethylenes alike by a single Shultz–Flory plot provided the usual abcissa ($m_w^{-1/2}$) is replaced by $[\eta]^{-1}$. It is hard to conceive a theoretical foundation for this, but the procedure evidently works well. Measurements of second virial coefficients as a function of temperature will be needed to clarify the situation.

The distribution coefficient of each species as a function of molar mass can be deduced from the data available now. We postpone dealing with this information also, because in this respect even linear chains have so far escaped quantitative treatment.

Although for convenience the parameter ϵ was described as measuring the effectivity of the end segments, the form of eq 10 allows a more general interpretation. This arises because the number of end segments concerned is in a one-to-one correspondence to the number of side branches. Accordingly, ϵ could model any kind of energy contribution proportional to the number of side branches. Such a contribution would in any case rapidly converge as the side branches get longer, as was implicitely postulated for ϵ.

Acknowledgment. The authors are indebted to their colleagues in the Fundamental Polymer Research Department (DSM) for the characterization of the polyethylene samples (GPC, LALLS, $[\eta]$, M_n, M_w, M_z) and for assistance in the measurements, to Mr. A. Veermans, who supplied the infrared data, and to Mr. H. Schepers, who prepared the hydrogenated polybutadiene sample.

References and Notes

(1) L. A. Kleintjens, H. M. Schoffeleers, and R. Koningsveld, *Ber. Bunsenges. Phys. Chem.*, **81** (10), 980 (1977).
(2) B. H. Zimm and W. H. Stockmayer, *J. Chem. Phys.*, **17**, 1301 (1949).
(3) T. A. Orofino and F. Wenger, *J. Phys. Chem.*, **67**, 566 (1963).
(4) G. C. Berry, *J. Polym. Sci., Part A-2*, **9**, 687 (1971).
(5) J. W. Kennedy, M. Gordon, and R. Koningsveld, *J. Polym. Sci., Part C*, **39**, 43 (1972).
(6) S. Nakano, *J. Polym. Sci., Polym. Phys. Ed.*, **12**, 1499 (1974).
(7) A. R. Shultz and P. J. Flory, *J. Am. Chem. Soc.*, **75**, 3881 and 5631 (1953).
(8) F. A. Bovey, F. C. Schilling, F. L. Mc Crackin, and M. L. Wagner, *Macromolecules*, **9**(1), 76 (1976).
(9) A. J. Staverman, *Recl. Trav. Chim. Pays-Bas*, **56**, 885 (1937).
(10) M. L. Huggins, *J. Phys. Chem.*, **74**, 371 (1970); **75**, 1255 (1971); **80**, 1317 (1976).
(11) P. J. Flory, *J. Am. Chem. Soc.*, **87**, 1833 (1965).
(12) H. Höcker, H. Shih, and P. J. Flory, *Trans. Faraday Soc.*, **67**, 2275 (1971).
(13) L. A. Kleintjens, R. Koningsveld, H. A. G. Chermin, and M. L. Huggins, *Br. Polym. J.*, **9**(3), 234 (1977).
(14) (a) J. S. Rowlinson, "Liquids and Liquid Mixtures", Butterworths, London, 1959, p 304; (b) G. Kanig, *Kolloid Z. Z. Polym.*, **190**, 1 (1963); **233**, 829 (1969).
(15) E. A. Guggenheim, "Mixtures", Claredon Press, Oxford, 1952.
(16) G. Rehage, *Kunststoffe*, **53**, 605 (1963).
(17) P. J. Flory, *J. Chem. Phys.*, **10**, 51 (1942); **12**, 425 (1944).
(18) M. L. Huggins, *Ann. N.Y. Acad. Sci.*, **43**, 1 (1942).
(19) A. J. Staverman and J. H. van Santen, *Recl. Trav. Chim. Pays-Bas*, **60**, 76 and 640 (1941).
(20) J. W. Gibbs, "Collected Works", Vol. I, Dover, New York, 1961.
(21) R. Koningsveld and L. A. Kleintjens, *Macromolecules*, **4**(5), 637 (1971).
(22) F. Zernike, Thesis, Amsterdam, 1915, and *Arch. Neerl. Sci., Exactes Nat., Ser 3A*, **4**, 74 (1918).
(23) H. C. Brinkman and J. J. Hermans, *J. Chem. Phys.*, **17**, 574 (1949).
(24) W. H. Stockmayer, *J. Chem. Phys.*, **18**, 54 (1950).
(25) P. J. Debye, *J. Chem. Phys.*, **31**, 680 (1959).
(26) B. Chu, F. J. Schoenes, and M. E. Fisher, *Phys. Rev.*, **185**, 219 (1969).
(27) Th. G. Scholte, *J. Polym. Sci., Part A-2*, **9**, 1553 (1971); *J. Polym. Sci., Part C*, **39**, 281 (1972).
(28) J. Goldsbrough, *Sci. Prog. (Oxford)*, **60**, 281 (1972).
(29) M. Gordon, J. Goldsbrough, B. W. Ready, and K. Derham in "Industrial Polymers", J. H. S. Green and R. Dietz, Eds., Transcripta Books, London, 1973, p 45.
(30) K. Derham, J. Goldsbrough, and M. Gordon, *Pure Appl. Chem.*, **38**, 97 (1974).
(31) R. Koningsveld, W. H. Stockmayer, J. W. Kennedy, and L. A. Kleintjens, *Macromolecules*, **7**, 73 (1974).
(32) R. Koningsveld, Ph.D. Thesis, Leiden, 1967; R. Koningsveld and A. J. Staverman, *Kolloid Z. Z. Polym.*, **218**, 114 (1967).
(33) R. Koningsveld, L. A. Kleintjens, and A. R. Schultz, *J. Polym. Sci., Part A-2*, **8**, 1261 (1970).
(34) G. V. Schulz and B. Jirgensons, *Z. Phys. Chem., B*, **46**, 105 (1940).
(35) H. Okamoto, *J. Phys. Soc. Jpn.*, **14**, 1388 (1959).
(36) J. W. Breitenbach and B. Wolf, *Makromol. Chem.*, **108**, 263 (1967).
(37) G. Rehage, D. Moller, and O. Ernst, *Makromol. Chem.*, **88**, 232 (1965).
(38) L. A. Kleintjens, R. Koningsveld, and W. H. Stockmayer, *Br. Polym. J.*, **8**, 144 (1976).
(39) W. Ball and Th. Scholte, *Pure Appl. Chem.*, **50**, 1715 (1978).
(40) L. A. Kleintjens, Thesis, Essex, 1979.
(41) R. Chiang, *J. Phys. Chem.*, **69**, 1645 (1965).
(42) A. Nakajima, US–Japan Joint Seminar on Polymer Physics, Kyoto, 1965.
(43) H. Schepers, private communication.
(44) M. Gordon and P. Irvine, *Polymer*, in press.